Since January 2020 Elsevier has created a COVID-19 resource centre with free information in English and Mandarin on the novel coronavirus COVID-19. The COVID-19 resource centre is hosted on Elsevier Connect, the company's public news and information website.

Biosensors and Bioelectronics 199 (2022) 113883

Contents lists available at ScienceDirect

Biosensors and Bioelectronics

journal homepage: www.elsevier.com/locate/bios

Dual-detection fluorescent immunochromatographic assay for quantitative detection of SARS-CoV-2 spike RBD-ACE2 blocking neutralizing antibody

Xuejun Duan [a,1,*], Yijun Shi [b,d,e,1], Xudong Zhang [a], Xiaoxiao Ge [c], Rong Fan [a], Jinghan Guo [a], Yubin Li [a], Guoge Li [b,d,e], Yaowei Ding [b,d,e], Rasha Alsamani Osman [b,d,e], Wencan Jiang [b,d,e], Jialu Sun [b,d,e], Xin Luan [b,d,e], Guojun Zhang [b,d,e,**]

[a] Beijing North Institute of Biotechnology Co., Ltd., NO. A20 Panjiamiao, Fengtai Distrct, Beijing, China
[b] Department of Clinical Diagnosis, Laboratory of Beijing Tiantan Hospital, Capital Medical University, Beijing, China
[c] Beijing Institute of Brain Disorders, Capital Medical Univerity, Beijing, China
[d] NMPA Key Laboratory for Quality Control of In Vitro Diagnostics, Beijing, China
[e] Beijing Engineering Research Center of Immunological Reagents Clinical Research, Beijing, China

ARTICLE INFO

Keywords:
Dual-detection
Ratiometric biosensor
SARS CoV-2
Neutralization antibody
Lateral flow assay
Point of care testing

ABSTRACT

The global effort against the COVID-19 pandemic dictates that routine quantitative detection of SARS-CoV-2 neutralizing antibodies is vital for assessing immunity following periodic revaccination against new viral variants. Here, we report a dual-detection fluorescent immunochromatographic assay (DFIA), with a built-in self-calibration process, that enables rapid quantitative detection of neutralizing antibodies that block binding between the receptor-binding domain (RBD) of the SARS-CoV-2 spike protein and the angiotensin-converting enzyme 2 (ACE2). Thus, this assay is based on the inhibition of binding between ACE2 and the RBD of the SARS-CoV-2 spike protein by neutralizing antibodies, and the affinity of anti-human immunoglobulins for these neutralizing antibodies. Our self-calibrating DFIA shows improved precision and sensitivity with a wider dynamic linear range, due to the incorporation of a ratiometric algorithm of two-reverse linkage signals responding to an analyte. This was evident by the fact that no positive results (0/14) were observed in verified negative samples, while 22 positives were detected in 23 samples from verified convalescent plasma. A comparative analysis of the ability to detect neutralizing antibodies in 266 clinical serum samples including those from vaccine recipients, indicated that the overall percent agreement between DFIA and the commercial ELISA kit was 90.98%. Thus, the proposed DFIA provides a more reliable and accurate rapid test for detecting SARS-CoV-2 infections and vaccinations in the community. Therefore, the DFIA based strategy for detecting biomarkers, which uses a ratiometric algorithm based on affinity and inhibition reactions, may be applied to improve the performance of immunochromatographic assays.

1. Introduction

SARS-CoV-2 neutralizing antibodies protect against SARS-CoV-2 viral infections by blocking cellular infiltration and replication via binding to the pathogen (Khoury et al., 2021; Shi et al., 2020). Evidently, the use of neutralizing antibodies from the blood of convalescent patients is critical for implementing a plasma-based therapeutic approach against SARS-CoV-2 (Hoffmann et al., 2020). The receptor-binding domain (RBD) of the SARS-CoV-2 virus spike protein (S protein) is essential for virus infiltration, and utilizing antibodies against the RBD of SARS-CoV-2 appears to exert a protective effect on convalescent patients (Ou et al., 2020; Premkumar et al., 2020). Many vaccines induce the generation of neutralizing antibodies, which effectively block the interaction between the RBD and its receptor, angiotensin converting enzyme 2 (ACE2), on the host cell (Wang, 2021). The levels of these neutralizing antibodies act as effective predictors of immune protection (Bergwerk et al., 2021) and also enable the development of vaccine strategies against COVID-19 (Tan et al., 2020), with particular

* Corresponding author. Beijing North Institute of Biotechnology Co., Ltd., NO. A20, Panjiamiao, Fengtai Distrct, Beijing, China.
** Corresponding author. Beijing Tiantan Hospital, Capital Medical University, No.119 South Fourth Ring West Road, Fengtai District, Beijing, China.
E-mail addresses: xzs_duanxuejun@163.com (X. Duan), tiantanzgj@163.com (G. Zhang).
[1] These authors contributed equally.

https://doi.org/10.1016/j.bios.2021.113883
Received 21 September 2021; Received in revised form 3 December 2021; Accepted 9 December 2021
Available online 15 December 2021

reference to future periodic revaccinations against new viral variants (Le, 2021), such as Delta (Chmielewska et al., 2021) and Omicron variants. The neutralizing antibody against SARS-CoV-2 is tested by evaluating its ability to inhibit binding between SARS-CoV-2 RBD and ACE2. A SARS-CoV-2 surrogate virus neutralization competition ELISA and a surface plasmon resonance assay (SPR), which are based on this principle, have been developed recently (Walker et al., 2020). A serological ELISA kit was authorized by the US FDA. Compact and portable biosensors and electrochemical point-of-care systems for specific antibody against infectious diseases, including the emerging digital microfluidic systems, have also been developed recently (Ng et al., 2018; Mahshid et al., 2021; Torres et al., 2021). However, the need for rapid, as well as routinely and broadly accessible point-of-care immunosensors that can be used to quantitatively detect and screen neutralizing antibodies against SARS-CoV-2 and its new variants is urgently felt.

Self-testing for COVID-19 using immunochromatographic assays, also known as lateral flow assays, is widespread. Common rapid serological tests that detect SARS-CoV-2 antibody levels in circulation usually employ gold nanoparticle- or fluorescent reporter-labeled recombinant SARS-CoV-2 antigen and anti-human immunoglobulin coated test lines (Liu et al., 2021; Peng et al., 2021). Other rapid methods that involve the labeling of anti-human immunoglobulins and recombinant SARS-CoV-2 antigen coating in test lines have been developed (Chen et al., 2020; Roda et al., 2021). A double-antigen sandwich lateral flow assay that detects SARS CoV-2 specific total antibody has been developed (Cavalera et al., 2021). However, a rapid immunochromatographic assay for neutralizing antibodies against SARS-CoV-2, that enables routine and broadly accessible quantitative detection is still lacking (Lake et al., 2020; Wang et al., 2021a,b; Zhang et al., 2020).

Traditional quantitative immunochromatographic assays measure analyte concentrations by collecting single-signal response data on one test line. Because this single signal method is easily affected by interference from various factors unrelated to the target (Guo et al., 2021; Hou et al., 2020), the accuracy and sensitivity of quantitative immunochromatographic assays remain unsatisfactory. However, dual-signal ratio bioassays provide higher precision and sensitivity than single-signal measurements (Park et al., 2020; Shen et al., 2020; Spring et al., 2021). The classical ratiometric fluorescence assay uses one fluorescence intensity change as a reference to standardize the other changes that occur in response to the same analyte at different wavelengths, thereby providing a built-in self-calibration signal readout. However, only a few reports on the application of these types of ratio principle of fluorescence assays to immunochromatographic assays are currently available (Wang et al., 2021a,b).

In the current study, we designed a new dual-detection fluorescent immunochromatographic assay (DFIA), which measures the concentration of neutralizing antibodies via a ratiometric algorithm of two-reverse linkage detection signals responding to the same analyte on two separate test lines. To the best of our knowledge, our study is the first to apply ratiometric fluorescent analysis to immunochromatographic assays.

2. Materials and methods

2.1. Immunoreagents, chemicals materials and samples

Recombinant SARS CoV-2 spike protein receptor-binding domain (RBD) (Cat: 40592-V05H) and recombinant human receptor angiotensin converting enzyme 2 (ACE2) (Cat:10108-H08H) were purchased from Sino Biological Inc (Beijing, China). Goat anti-human IgG and IgM and IgA antibodies (ab102416) were purchased from Abcam (Cambridge, England). Carboxyl-functionalized Europium chelate nanoparticles (EuNPs) (Catalog Number FCEU001) were obtained from Bangs Laboratories (IN, USA). Lateral Flow Nitrocellulose membranes (Vivid 120) were obtained from Pall Corporation (Washington, NY,USA). Glass fiber conjugate pads, adsorbent pads, and blood separator sample pads were purchased from Shanghai Kinbio Tech. Co., Ltd (Shanghai, China). Bovine serum albumin (BSA) was supplied by Roche (Basel, Switzerland). Mouse anti-human-RBC antibodies were obtained from Eastmo Biotech Co., Ltd (Beijing, China). 2-(N-morpholino) ethanesulfonic acid (MES), polyvinylpyrrolidone 10 (PVP10), 1-ethyl-3-(3-(dimethylamino) propyl) carbodiimide hydrochloride (EDC), and Proclin-300 were obtained from Sigma-Aldrich (St. Louis, MO, USA). N-Hydroxy-sulfosuccinimide (sulfo-NHS) was obtained from Thermo Fisher Scientific (Waltham, MA USA). Blockmaster™ PA1080 was obtained from the JSR Life Sciences (Sunnyvale, CA, USA). Tween 20 and other chemicals were purchased from Sinopharm. Amicon Ultra Centrifugal Filter Units (10 kDa) were obtained from Merck Millipore (Billerica, MA, USA). The ELISA kit was a blocking ELISA detection assay for the detection of neutralizing antibodies (cPass SARS-CoV-2 Neutralization Antibody Detection Kit, GenScript USA Inc.) (Piscataway, NJ, USA). The first WHO International Standard for anti-SARS-CoV-2 immunoglobulin, human (NIBSC code:20/136), First WHO International Reference Panel for anti-SARS-CoV-2 immunoglobulin, human (NIBSC code: 20/268), and Anti-SARS-CoV-2 Verification Panel for Serology Assay were obtained from the National Institute for Biological Standards and Control (NIBSC), UK.

The solutions were prepared as following: coating buffer (0.5% trehalose [w/v] and 10% SeaBlock [v/v] in 50 mM borate-boric acid buffer, pH 8.5); sample pad pre-treatment buffer (1.5 μg/mL mouse anti human-RBC antibody, 0.02% Tween-20 [v/v], 0.9% NaCl [w/v] in 50 mM Tris-HCl, pH8.0); conjugate buffer (8% trehalose [w/v], 1% PVP10 [w/v], 3% D-mannitol [w/v], and 0.1% BSA [w/v] in 50 mM borate-boric acid buffer, pH 8.5), activation buffer (50 mM MES, pH 5.4), coupling buffer (50 mM borate-boric acid buffer, pH 8.5), and sample diluent (0.02% Tween-20 [v/v], 0.45% NaCl [w/v], 0.3% Blockmaster™ PA1080 [w/v] in 50 mM Tris-HCl, pH 7.8).

FIC-H1W dry fluorescence immunoassay analyzer was obtained from Suzhou Helmen Precision Instruments Co., Ltd. (Suzhou, Jiangsu, China).

Serum samples were obtained from Beijing Tiantan Hospital Capital Medical University. This study was approved by the Beijing Tiantan Hospital Capital Medical University (Beijing, China) (ethics approval number: KY2021-132-02).

2.2. Conjugation of SARS CoV-2 RBD antigens to Europium chelate nanoparticles

The SARS CoV-2 RBD and chicken IgY antigen (for the control test) were conjugated to EuNPs via a two-step procedure. Briefly, 5 μL of EuNPs (1% w/v) was washed in 1 mL of activation buffer, centrifuged at 12000 g for 30 min, and resuspended in activation buffer (0.5 mL). Two microliters of EDC (0.5 mg/mL EDC [w/v] in activation buffer) and 2 μL of sulfo-NHS (0.5 mg/mL sulfo-NHS [w/v] in activation buffer) were added to activate the EuNPs and mixed for 15 min with gentle rotation at room temperature. After washing again, followed by centrifugation at 12000*g* for 30 min with coupling buffer, the activating EuNPs were ultrasonically resuspended in coupling buffer (0.5 mL).

The SARS CoV-2 RBD and chicken IgY antigen were desalted and transferred to coupling buffer at a concentration of 2 mg/mL by ultrafiltration; 20 μg of as-prepared SARS CoV-2 RBD and 20 μg of chicken IgY antigens were added to the activated nanoparticles resuspended in coupling buffer. Following 2 h of incubation at 22 °C with gentle rotation, 50 μL of 5% (w/v) BSA was added and further incubated at 22 °C with gentle rotation for 2 h. The RBD or chicken IgY antigen-conjugated EuNPs were centrifugated at 12000 g for 30 min, resuspended in 1 mL conjugate buffer, and then mixed, producing 2 mL of conjugated EuNPs in conjugate buffer.

2.3. Fabrication of the dual-detection fluorescence immunochromatographic assay strips

The prepared 2 mL of conjugated EuNPs in conjugate buffer were dispensed on glass fiber conjugate pads (1.8 mm*300 mm) and dried at 37 °C for 2 h. The sample pad was saturated with sample pad pre-treatment buffer and dried at 37 °C for 2 h.

Nitrocellulose membranes were laminated onto a backing card. Recombinant human ACE2 and goat anti-human IgG and IgM and IgA antibodies were diluted with coating buffer at assigned concentrations and dispensed onto a nitrocellulose membrane on the backing card at 1 μL/cm per test 1 line (T1) and test 2 line (T2). Goat anti-chicken IgY was also diluted with coating buffer at a concentration of 1 mg/mL and dispensed onto a nitrocellulose membrane at 1 μL/cm as control lines (C). The membrane was then dried at 37 °C for 2 h. The absorbent pad, the conjugate pad, and the sample pad were sequentially overlapped onto a backing card (Fig. 1a). Four millimeters wide strips , which contained 0.3 μg of labeled RBD per strip , were cut and fabricated in plastic cassettes. The cassettes were stored in a sealed aluminum foil bag with a desiccant silica gel at room temperature until use. The total cost is less than five US dollars per cassette.

2.4. Detection of SARS CoV-2 RBD-ACE2 blocking neutralization antibody by DFIA and commercial ELISA kit

Serum samples were detected using a serological ELISA kit (cPass SARS-CoV-2 Neutralization Antibody Detection Kit, GenScript USA Inc.) according to the manufacturer's instructions, and classified as positive when the inhibition rates were higher than the cut-off level of 20%.

DFIA for the SARS CoV-2 RBD-ACE2 blocking antibody was carried out at room temperature. Briefly, 10 μL of serum, or 20 μL whole blood, was added to the sample well of the cassette, following which 80 μL of sample diluent was applied to the sample well. Following a migration period of 15 min, the cassette was loaded into a portable fluorescence

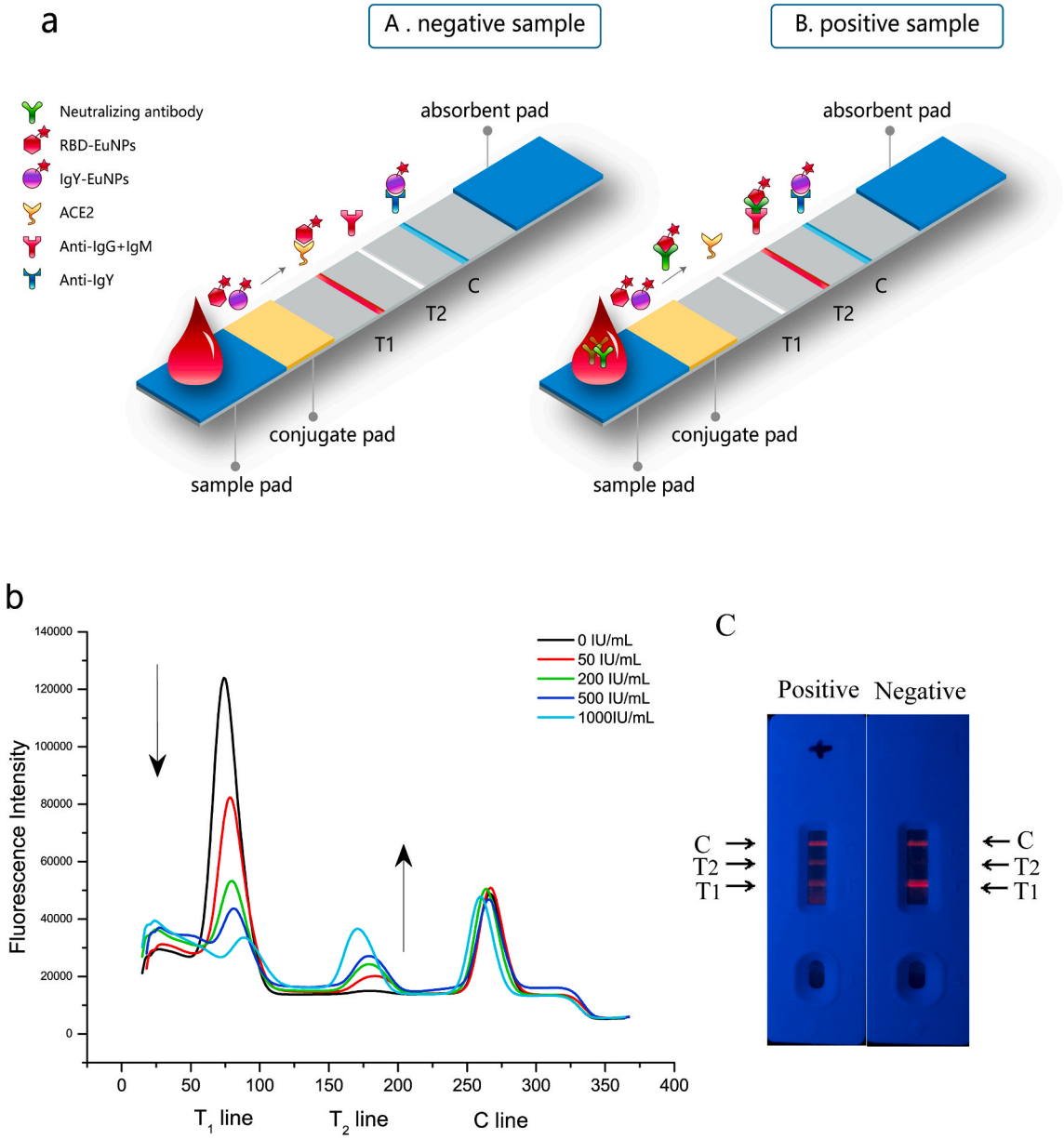

Fig. 1. (a) Scheme of dual-detection fluorescent immunochromatographic assay for the SARS CoV-2 RBD-ACE2 blocking antibody. (b) Two-reverse linkage fluorescence response signal towards different concentrations of the SARS CoV-2 RBD-ACE2 blocking neutralization antibody. (c) Positive and negative samples tested using the DIFA cassette.

reader (excitation wavelength, 365 nm; emission wavelength, 615 nm). The fluorescence peak area of T1, T2, and the control line (C) was measured respectively (Fig. 1). The ratio (R) was calculated as follows: R = T2/(T1+T2).

The calibration curve of DFIA for RBD-ACE2 blocking antibodies (Fig. 3) was constructed using known antibody concentrations (in IU/mL) as the abscissa (x value) and (R) as the ordinate (y value). Positive and negative serum samples were collected and used to prepare a working calibrator. Working calibrators were then standardized according to the First WHO International Standard for anti-SARS-CoV-2 immunoglobulin (NIBSC code: 20/136).

3. Results and discussion

3.1. Design and performance of the SARS CoV-2 RBD-ACE2 blocking neutralization antibody DFIA

In this study, we developed a dual-detection fluorescent

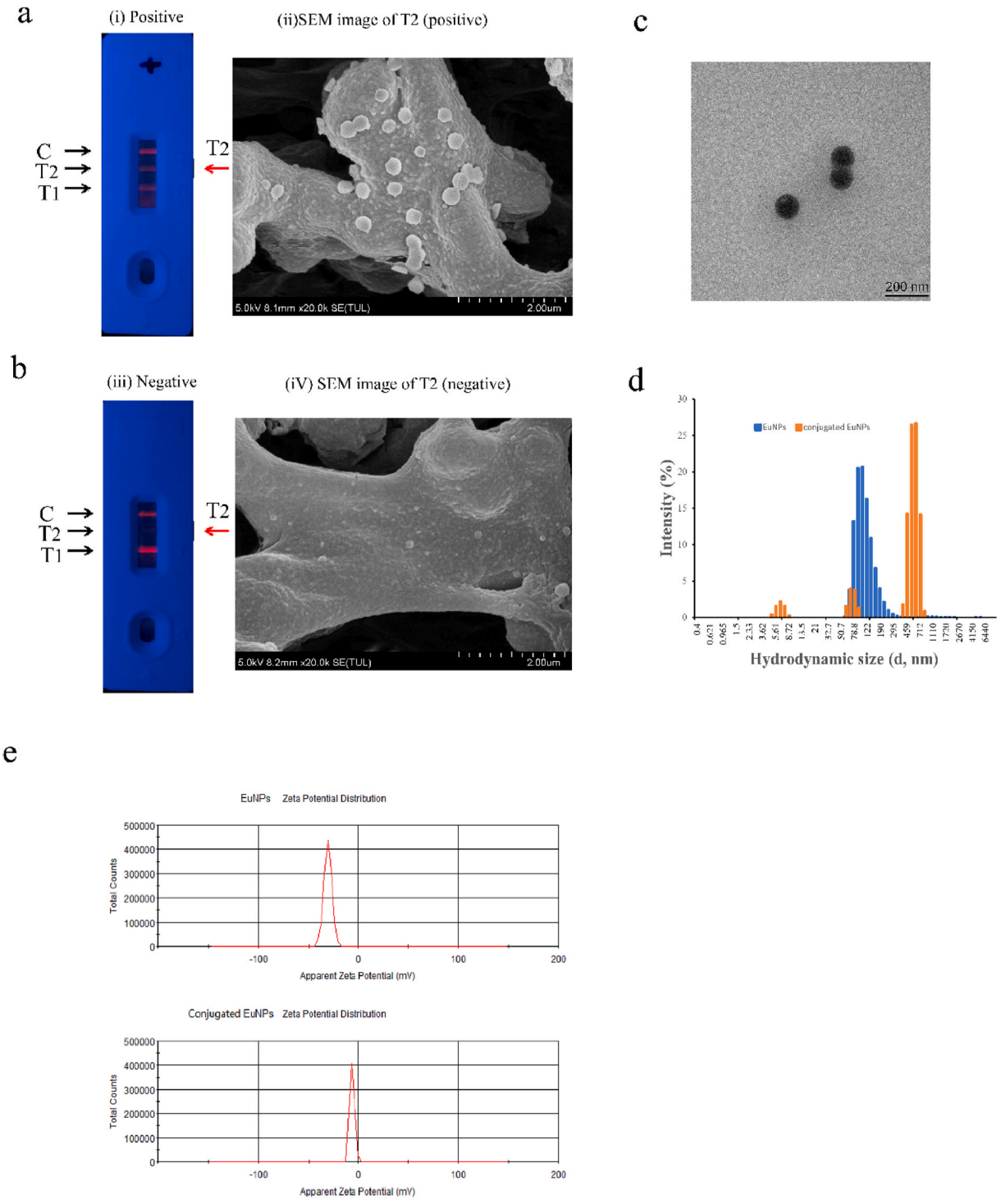

Fig. 2. Characterization of EuNPs and conjugated EuNPs. (a) Positive assay: (i) fluorescence photographs and (ii) its SEM image of T2. (b) Negative assay: (iii) fluorescence photographs and (iv) its SEM image of T2. (c) TEM image of conjugated EuNPs. (d) Hydrodynamic size distribution of EuNPs and conjugated EuNPs. (e) Surface zata potential of EuNPs and conjugated EuNPs.

immunochromatographic assay (DFIA) that measures not only the inhibition of the SARS CoV-2 RBD-ACE2 blocking antibody, which blocks the RBD-conjugated reporter from binding to ACE2, but also the concentration of the neutralizing antibodies bound to the RBD conjugated reporter (Fig. 1a). Furthermore, we observed that the signal of the T1 line always increased as the intensity of the T2 line decreased, and vice versa (Fig. 1b and c). The instrument was permitted to report effective measurement results only when the requirements of the above-mentioned signal characteristics were met. In this manner, the chances of false positives or false negatives occurring due to interference

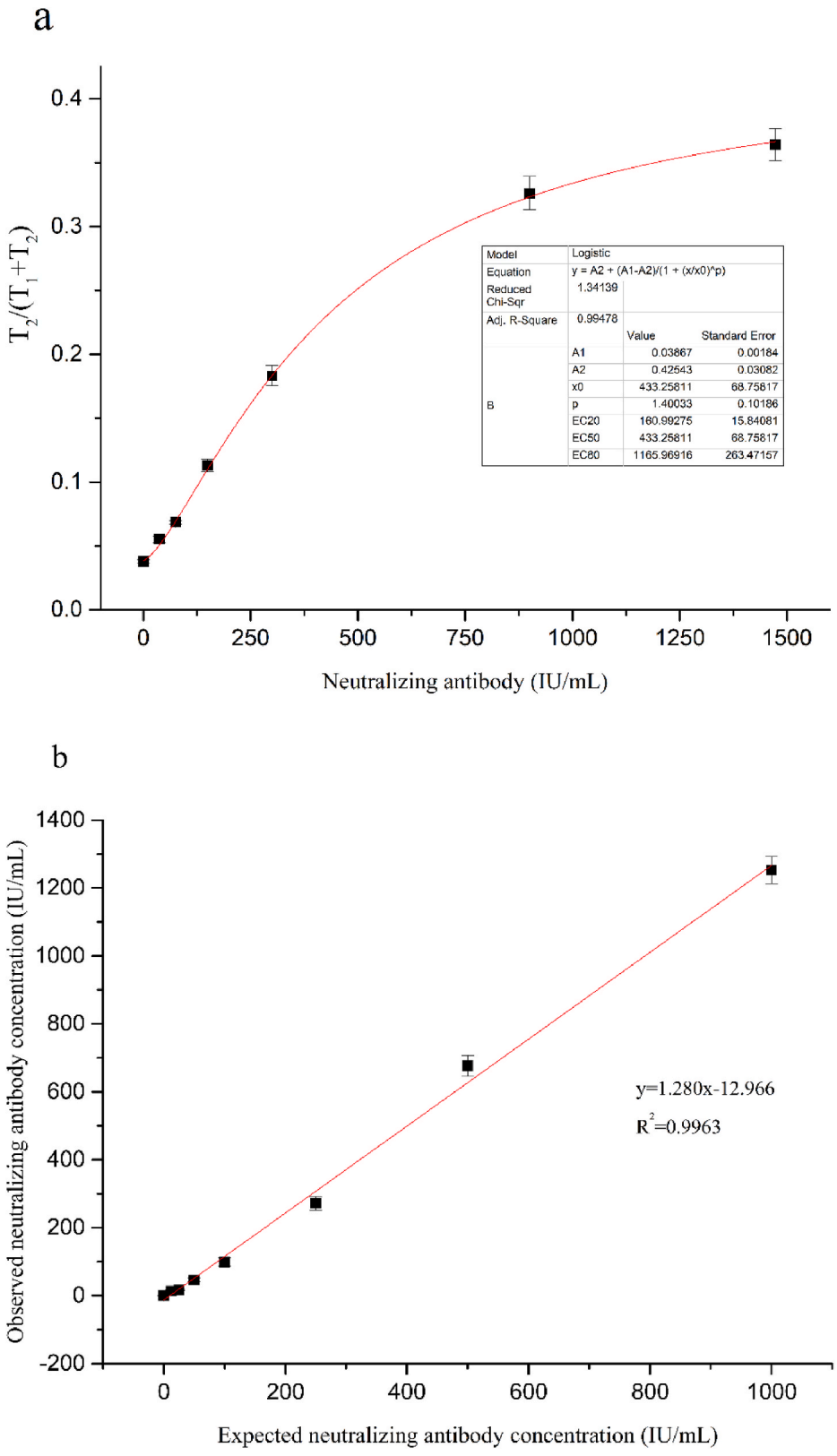

Fig. 3. (a) Calibration curve, and (b) Dilution linearity of the SARS CoV-2 RBD-ACE2 blocking neutralization antibody DFIA.

could be reduced.

When the test sample migrated from the sample pad toward the absorbent pad, SARS CoV-2 RBD-ACE2 blocking antibody, if present in the samples, binds to the rehydrating RBD-conjugated nanoparticles to form an immune complex, thereby blocking any interaction between ACE2 coated in the T1 line and RBD-conjugated nanoparticles. The intensity of the T1 line is inversely proportional to the concentration of the neutralizing antibodies (Fig. 1b and c). Because the neutralizing antibodies bound to the RBD-conjugated reporter continue to migrate along the strip until they are captured by goat anti-human IgG and IgM and IgA immobilized on the T2 line, the intensity of the T2 line is positively proportional to the concentration of neutralizing antibodies. The control, consisting of unbound chicken IgY antigen-conjugated nanoparticles, continues to migrate alone until these are captured in the control line (C), indicating the validity of the test.

3.2. Characterization of EuNPs and conjugated EuNPs

Scanning electron microscopy (SEM) images showed the conjugated EuNPs captured in the T2 line of positive (Fig. 2a ii) and not captured in T2 line of negative (Fig. 2b iv) assay respectively. The conjugated EuNPs were also characterized by transmission electron microscopy (TEM) (Fig. 2c). The dynamic light scattering analysis (DLS) showed that the hydrodynamic sizes were changed when the EuNPs were conjugated (Fig. 2d). The surface zeta potential of EuNPs and conjugated EuNPs (Fig. 2e) were -30.5 ± 0.2 mv and -6.5 ± 0.2 mv respectively. These data indicated that conjugated EuNPs had been functionalized.

3.3. Calibration curve of the SARS CoV-2 RBD-ACE2 blocking neutralization antibody DFIA

Plotting of the calibration curve of our proposed DFIA method was based on the concentrations of SARS CoV-2 RBD-ACE2 blocking antibody calibrators (S0–S6) and the corresponding dose–response mean values of the obtained ratio (R) of T2/(T1+T2). In this study, some results of the neutralization antibody assay did not fall within the linear portion of the dose–response curve, but can be fitted well with data under 4 PL logistic regression analysis (see Fig. 3a). Thus, we processed the immunoassay data as recommended general form of equation (Dudley et al., 1985; Dunn and Wild, 2013), which was $y = A2 + (A1 - A2)/[1 + (x/x_0)\ ^\wedge p]$ (correlation coefficient (R^2) = 0.9948), where A1= 0.0387, A2 =0.425, p =1.400, x_0= 433.258.

3.4. Optimization of DFIA for the SARS CoV-2 RBD-ACE2 blocking neutralization antibody

In order to optimize assay time, the R (T2/(T1+T2)) of two positive samples and one negative sample was measured every 1 min over a period of 0–20 min starting from the beginning of the assay. R increased rapidly over the first 4 min and reached a plateau at 15 min (Fig. S1(a)). Based on this result, total assay time was set to 15 min.

We compared different amounts of labeled RBD (0.15, 0.3, 0.45, 0.6 and 0.75 μg of labeled RBD per strip) fabricated in the conjugated pad. Subsequently, we selected 0.3 μg of labeled RBD per strip, which R of positive sample reached its highest value (Fig. S1(b)).

To optimize the concentration of ACE2 coated on test line 1, we compared the performances of 0.25, 0.5 and 1.0 mg/mL of ACE2 by using these concentrations to test a positive sample. Both the inhibition of neutralizing antibodies and the R value were highest when the concentration of ACE2 coated on Test 1 line was 0.5 mg/mL (Fig. S1c). Therefore, a coated concentration of 0.5 mg/mL ACE2 was chosen. Furthermore, 1 mg/mL of anti-human IgG and IgM and IgA coated on test line 2 was sufficient to capture almost all neutralizing antibodies in 10 μL serum.

3.5. The DFIA displayed improved performances in limit of blank (LOB), limit of detection (LOD), linearity, precision, and accuracy compared with the classical (T/C) method

We calculated the mean and standard deviation (SD) of R using 20 replicates of the negative sample. The LOB calculated as mean + 1.64 (SD) was 3.01 IU/ml according to the calibration curve. The SD of the low concentration sample of S2 was calculated using the measured values from 20 replicates. The LOD of our proposed DFIA was defined as the concentration converted from LOD = LOB +1.645 (SD_{S2}), and yielded 7.6 IU/mL according to the DFIA calibration curve. In contrast, the LOD for the T1/C method was 13.4 IU/mL according to the calibration curve of T1/C, while the LOD for the T2/C method was 38.3 IU/mL. These findings indicated that DFIA showed improved sensitivity to CoV-2 RBD-ACE2 blocking neutralization antibodies.

The dual detection ratiometric algorithm, R = T2/(T1+T2), significantly improved precision, compared with the single signal T/C method used in classical lateral flow assays. Both intra-assay and inter-assay coefficients of variation were below 15% (Table S1). We measured two serum samples using ten replicates per day for five consecutive days. The inter-assay coefficient of variation (5.5%–10.1%) of the ratiometric algorithm, T2/(T1+T2), was much superior to that of the T/C method (13.4%–18.4%); (Table S1), because it was lower.

According to the CLSI guideline EP06-A, regression analysis was used to compare expected and observed SARS CoV-2 RBD-ACE2 blocking antibody concentrations in serial dilution samples. It showed linearity (R2=0.996) in the range of 12.5–1000 IU/mL for the proposed assay (Fig. 3b). Two serum samples assigned as 75 IU/mL and 500 IU/mL, were prepared using negative samples according to the First WHO International Standard for anti-SARS-CoV-2 immunoglobulin, human (NIBSC code: 20/136) and then measured in triplicate using our proposed DFIA. The percent recovery was 102.9% (75 IU/mL) and 88.1% (500 IU/mL), respectively.

3.6. Comparison of the performances of DFIA and the commercial ELISA in detecting neutralization antibodies in clinical samples

A total of 266 serum samples collected from persons with no history of 2019-nCoV pneumonia was used to detect SARS CoV-2 RBD-ACE2 blocking antibodies. Of these 266 serum samples, 128 were obtained from a population that was physically examined before June 2019, while 138 were obtained from people who had two doses of Sinovac COVID-19 vaccine.

Serum samples were first analyzed using a serological ELISA kit (cPass SARS-CoV-2 Neutralization Antibody Detection Kit, GenScript USA Inc.), which registered as an Emergency Use Authorization (EUA) kit by the US Food and Drug Administration (FDA). This kit, which was used according to the manufacturer's instructions, indicated that the inhibition rates corresponding to 118 serum sample exceeded the cut-off level of 20% and could be classified as positive. The other 148 were classified as negative because their inhibition rates did not exceed the cut-off level.

The same serum samples were tested using our DFIA, wherein the concentration cut-off points of the RBD-ACE2 blocking antibody were analyzed using a receiver operating characteristic curve (ROC) with IBM SPSS Statistics 22. the cut-off value was 16 IU/mL, and the area under the ROC curve (AUC) was 0.955 (Fig. 4a).

Unlike the cPass SARS-CoV-2 Neutralization Antibody Detection Kit or other known analytical methods, which only measure the inhibition of the antibody, DFIA takes other factors, such as inhibition by RBD-ACE2 blocking antibodies and the quantity of RBD-ACE2 blocking antibodies, in to consideration. The degree of agreement between the results of DFIA and ELISA was $\kappa = 0.8166$ (95% CI (0.7467–0.88865); $p \leq .001$) analyzed with IBM SPSS Statistics 22. The overall percent agreement between DFIA and the commercial ELISA kit for detecting neutralizing antibodies in the 266 clinical serum samples, including

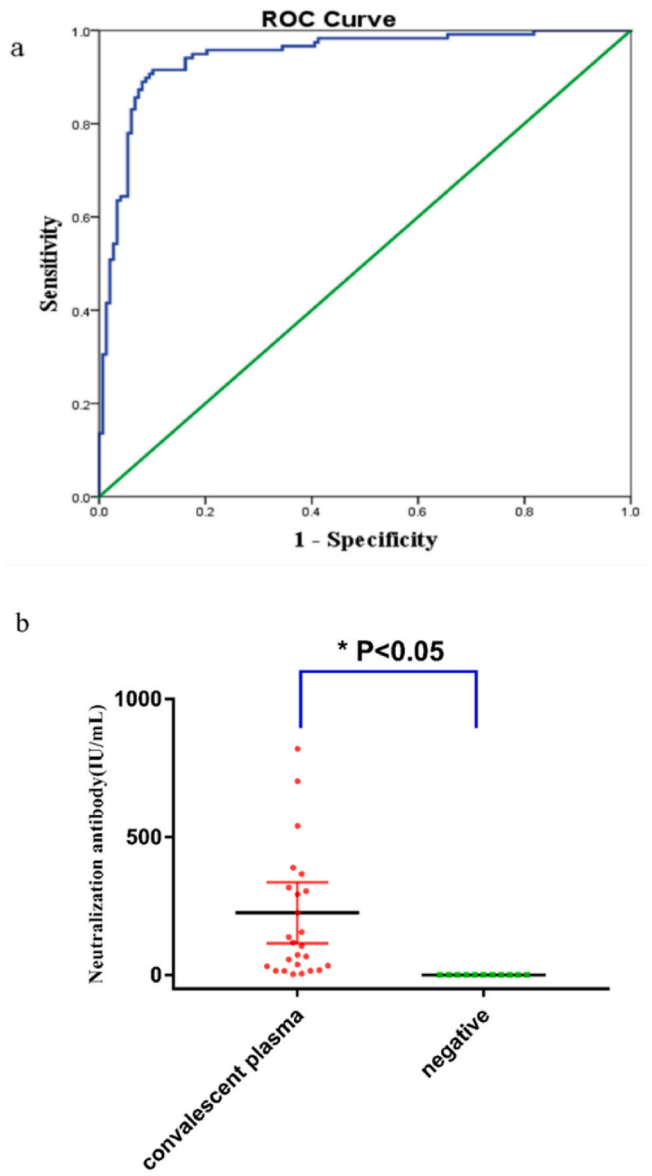

Fig. 4. (a) Receiver operating characteristic curve (ROC) of the SARS CoV-2 RBD-ACE2 blocking neutralization antibody DFIA. (b) Test results of Anti-SARS-CoV-2 Verification Panel by DFIA.

those from vaccine recipients, was 90.98% (86.87%～94.13%) (Table 1).

3.7. Assessment of neutralization antibodies using DFIA

We tested and calculated the percent recovery of neutralization antibodies from Reference Panel (NIBSC code: 20/268). The panel consisted of pooled plasma samples obtained from individuals who had recovered from Coronavirus Disease 2019) (COVID-19) and a negative control involving plasma obtained from healthy blood donors before 2019. The test results of our proposed method were in good agreement with the verified data (Table 2), not including NIBSC code 20/150 which was not fall within the linear range of 12.5–1000 IU/mL.

In order to validate the performance of DFIA in recovering neutralization antibodies, we also tested the Anti-SARS-CoV-2 Verification panel for Serology Assay from NIBSC (United Kingdom). Neutralization antibody test results obtained by DFIA are analyzed with GraphPad Prism 7.0(Fig. 4b). No false-positive results (0/14) were observed, and 22 out of 23 samples from convalescent plasma samples were positive. This indicated that our proposed DFIA for neutralization antibodies had met the standards required for studying immune response to SARS-CoV-2 vaccination or prior infection.

Table 1
Comparison of results obtained using DFIA and the commercial ELISA kit in clinical samples.

		DFIA		Total	Percent Agreement, %
		Positive	Negative		(95% CI)
ELISA	**Positive**	104	14	118	Positive:88.14(80.14～93.36)
	Negative	10	138	148	Negative:93.24(87.93～96.71)
	Total	114	152	266	Overall: 90.98(86.87～94.13)

4. Conclusions

A new dual-detection ratiometric analysis method was successfully designed and applied to a fluorescence immunochromatographic assay aimed at detecting SARS CoV-2 RBD-ACE2 blocking antibodies in human serum. Benefits associated with the self-calibration method which integrates two reverse response signal detection processes, enabled the proposed dual-detection fluorescence immunochromatographic assay (DFIA) to show a performance which was superior to that of the classical immunochromatographic assay. Furthermore, the newly introduced dual-detection ratiometric fluorescent analysis shows great potential for improving the performances of immunochromatographic assays involving other biomarkers.

The dual-detection fluorescence immunochromatographic assay for neutralizing antibodies has been validated by the Anti-SARS-CoV-2 Verification Panel and is traceable via the First WHO International Standard for anti-SARS-CoV-2 immunoglobulin, human (NIBSC code: 20/136). The results showed good agreement between DFIA and commercial ELISA methods in detecting neutralizing antibodies in clinical samples. Thus, this rapid assay may expectedly be used in studies investigating SARS-CoV-2 infections as well as in campaigns aimed at vaccinating the wider community.

Data availability statement

The key datasets used in this study are presented in Supplementary. Additional datasets generated and/or analyzed during the current study are available from the corresponding author on reasonable request.

Funding

This research was funded by China National Nuclear Corporation [Grant Number not available].

CRediT authorship contribution statement

Xuejun Duan: Conceptualization, Formal analysis, Methodology, for DFIA, Writing – original draft. **Yijun Shi:** Conceptualization, Resources, clinical samples and diagnosis, Investigation, for DFIA, Writing –

Table 2
Test results of WHO Reference Panel for neutralization antibody by DFIA.

NIBSC codes of Reference Panel	Verified Neutralizing antibody (IU/mL)	Test results (IU/mL)	Standard deviations	Percent recovery (%)
20/142	negative	0	/	/
20/140	44	37.77	3.00	85.83%
20/144	95	98.21	6.03	103.37%
20/148	210	208.23	28.25	99.16%

original draft. **Xudong Zhang:** Methodology, for DFIA, Funding acquisition. **Xiaoxiao Ge:** Writing – review & editing. **Rong Fan:** Methodology, for DFIA. **Jinghan Guo:** Methodology, for DFIA. **Yubin Li:** Funding acquisition, project management. **Guoge Li:** Resources, Methodology, for DFIA. **Yaowei Ding:** Resources, clinical samples and diagnosis, Methodology, for DFIA. **Rasha Alsamani Osman:** Resources, clinical samples and diagnosis, Methodology, for DFIA. **Wencan Jiang:** Resources, clinical samples and diagnosis, Methodology, for DFIA. **Jialu Sun:** Resources, clinical samples and diagnosis, Methodology, for DFIA. **Xin Luan:** Resources, clinical samples and diagnosis, Methodology, for DFIA. **Guojun Zhang:** Conceptualization, Formal analysis, Writing – review & editing, All authors have read and agreed to the published version of the manuscript.

Declaration of competing interest

The authors declare the following financial interests/personal relationships which may be considered as potential competing interests: Xuejun Duan, Xudong Zhang, Rong Fan, Jinghan Guo, and Yubin Li are employees of Beijing North Institute of Biotechnology Co., Ltd. All authors declare no other relevant affiliations or financial conflict with the subject matter or materials discussed in the manuscript. The authors have no other relevant affiliations or financial involvement with any organization or entity with a financial interest in or financial conflict with the subject matter or materials discussed in the manuscript apart from those disclosed.

Acknowledgments

The authors thank Dr. Hong Lv from Beijing Tiantan Hospital, Capital Medical University for collecting and checking the serum samples. Authors thank professor Dihua Shangguan from Institute of Chemistry, Chinese Academy of Sciences for their helping revision of manuscript. We would like to thank Editage (www.editage.cn) for English language editing.

Appendix A. Supplementary data

Supplementary data to this article can be found online at https://doi.org/10.1016/j.bios.2021.113883.

References

Bergwerk, M., Gonen, T., Lustig, Y., Amit, S., Lipsitch, M., Cohen, C., Mandelboim, M., Levin, E.G., Rubin, C., Indenbaum, V., Tal, I., Zavitan, M., Zuckerman, N., Bar-Chaim, A., Kreiss, Y., Regev-Yochay, G., 2021. N. Engl. J. Med. 385, 1474–1484. https://doi.org/10.1056/NEJMoa2109072.

Cavalera, S., Colitti, B., Rosati, S., Ferrara, G., Bertolotti, L., Nogarol, C., Guiotto, C., Cagnazzo, C., Denina, M., Fagioli, F., Di Nardo, F., Chiarello, M., Baggiani, C., Anfossi, L., 2021. Talanta 223, 121737. https://doi.org/10.1016/j.talanta.2020.121737.

Chen, Z., Zhang, Z., Zhai, X., Li, Y., Lin, L., Zhao, H., Bian, L., Li, P., Yu, L., Wu, Y., Lin, G., 2020. Anal. Chem. 92, 7226–7231. https://doi.org/10.1021/acs.analchem.0c00784.

Chmielewska, A.M., Czarnota, A., Bieńkowska-Szewczyk, K., Grzyb, K., 2021. NPJ Vacc. 6, 142. https://doi.org/10.1038/s41541-021-00404-6.

Dudley, R.A., Edwards, P., Ekins, R.P., Finney, D.J., McKenzie, I.G., Raab, G.M., Rodbard, D., Rodgers, R.P., 1985. Clin. Chem. 31, 1264–1271.

Dunn, J., Wild, D., 2013. Wild, D.B.T.-T.I.H.. In: Fourth, E. (Ed.), Chapter 3.6 - Calibration Curve Fitting. Elsevier, Oxford, pp. 323–336. https://doi.org/10.1016/b978-0-08-097037-0.00022-1.

Guo, J., Chen, S., Tian, S., Liu, K., Ni, J., Zhao, M., Kang, Y., Ma, X., Guo, J., 2021. Biosens. Bioelectron. 181, 113160 https://doi.org/10.1016/j.bios.2021.113160.

Hoffmann, M., Kleine-Weber, H., Schroeder, S., Krüger, N., Herrler, T., Erichsen, S., Schiergens, T.S., Herrler, G., Wu, N.H., Nitsche, A., Müller, M.A., Drosten, C., Pöhlmann, S., 2020. Cell 181, 271–280. https://doi.org/10.1016/j.cell.2020.02.052 e8.

Hou, F., Liu, H., Zhang, Y., Gao, Z., Sun, S., Tang, Y., Guo, H., 2020. New J. Chem. 44, 15498–15506. https://doi.org/10.1039/D0NJ03156A.

Khoury, D.S., Cromer, D., Reynaldi, A., Schlub, T.E., Wheatley, A.K., Juno, J.A., Subbarao, K., Kent, S.J., Triccas, J.A., Davenport, M.P., 2021. Nat. Med. 27, 1205–1211. https://doi.org/10.1038/s41591-021-01377-8.

Lake, D.F., Roeder, A.J., Kaleta, E., Jasbi, P., Periasamy, S., Kuzmina, N., Bukreyev, A., Grys, T., Wu, L., Mills, J.R., McAulay, K., Seit-Nebi, A., Svarovsky, S., 2020. medRxiv. https://doi.org/10.1101/2020.12.15.20248264, 2020.12.15.20248264.

Le, X.C., 2021. Anal. Chem. 93, 8379–8380. https://doi.org/10.1021/acs.analchem.1c02327.

Liu, H., Dai, E., Xiao, R., Zhou, Z., Zhang, M., Bai, Z., Shao, Y., Qi, K., Tu, J., Wang, C., Wang, S., 2021. Sensor. Actuator. B Chem. 329, 129196 https://doi.org/10.1016/j.snb.2020.129196.

Mahshid, S.S., Flynn, S.E., Mahshid, S., 2021. Biosens. Bioelectron. 176, 112905 https://doi.org/10.1016/j.bios.2020.112905.

Ng, A.H.C., Fobel, R., Fobel, C., Lamanna, J., Rackus, D.G., Summers, A., Dixon, C., Dryden, M.D.M., Lam, C., Ho, M., Mufti, N.S., Lee, V., Asri, M.A.M., Sykes, E.A., Chamberlain, M.D., Joseph, R., Ope, M., Scobie, H.M., Knipes, A., Rota, P.A., Marano, N., Chege, P.M., Njuguna, M., Nzunza, R., Kisangau, N., Kiogora, J., Karuingi, M., Burton, J.W., Borus, P., Lam, E., Wheeler, A.R., 2018. Sci. Transl. Med. 10, eaar6076 https://doi.org/10.1126/scitranslmed.aar6076.

Ou, X., Liu, Y., Lei, X., Li, P., Mi, D., Ren, L., Guo, L., Guo, R., Chen, T., Hu, J., Xiang, Z., Mu, Z., Chen, X., Chen, J., Hu, K., Jin, Q., Wang, J., Qian, Z., 2020. Nat. Commun. 11, 1620. https://doi.org/10.1038/s41467-020-15562-9.

Park, S.H., Kwon, N., Lee, J.H., Yoon, J., Shin, I., 2020. Chem. Soc. Rev. 49, 143–179. https://doi.org/10.1039/c9cs00243j.

Peng, T., Sui, Z., Huang, Z., Xie, J., Wen, K., Zhang, Y., Huang, W., Mi, W., Peng, K., Dai, X., Fang, X., 2021. Sensor. Actuator. B Chem. 331, 129415 https://doi.org/10.1016/j.snb.2020.129415.

Premkumar, L., Segovia-Chumbez, B., Jadi, R., Martinez, D.R., Raut, R., Markmann, A., Cornaby, C., Bartelt, L., Weiss, S., Park, Y., Edwards, C.E., Weimer, E., Scherer, E.M., Rouphael, N., Edupuganti, S., Weiskopf, D., Tse, L.V., Hou, Y.J., Margolis, D., Sette, A., Collins, M.H., Schmitz, J., Baric, R.S., de Silva, A.M., 2020. Sci. Immunol. 5 https://doi.org/10.1126/sciimmunol.abc8413.

Roda, A., Cavalera, S., Di Nardo, F., Calabria, D., Rosati, S., Simoni, P., Colitti, B., Baggiani, C., Roda, M., Anfossi, L., 2021. Biosens. Bioelectron. 172, 112765 https://doi.org/10.1016/j.bios.2020.112765.

Shen, Y., Wu, T., Zhang, Y., Ling, N., Zheng, L., Zhang, S.L., Sun, Y., Wang, X., Ye, Y., 2020. Anal. Chem. 92, 13396–13404. https://doi.org/10.1021/acs.analchem.0c02762.

Shi, R., Shan, C., Duan, X., Chen, Z., Liu, P., Song, J., Song, T., Bi, X., Han, C., Wu, L., Gao, G., Hu, X., Zhang, Y., Tong, Z., Huang, W., Liu, W.J., Wu, G., Zhang, B., Wang, L., Qi, J., Feng, H., Wang, F.S., Wang, Q., Gao, G.F., Yuan, Z., Yan, J., 2020. Nature 584, 120–124. https://doi.org/10.1038/s41586-020-2381-y.

Spring, S.A., Goggins, S., Frost, C.G., 2021. Molecules 26. https://doi.org/10.3390/molecules26082130.

Tan, C.W., Chia, W.N., Qin, X., Liu, P., Chen, M.I.-C., Tiu, C., Hu, Z., Chen, V.C.-W., Young, B.E., Sia, W.R., Tan, Y.J., Foo, R., Yi, Y., Lye, D.C., Anderson, D.E., Wang, L.F., 2020. Nat. Biotechnol. 38, 1073–1078. https://doi.org/10.1038/s41587-020-0631-z.

Torres, M.D.T., de Araujo, W.R., de Lima, L.F., Ferreira, A.L., de la Fuente-Nunez, C., 2021. Materials 4, 2403–2416. https://doi.org/10.1016/j.matt.2021.05.003.

Walker, S.N., Chokkalingam, N., Reuschel, E.L., Purwar, M., Xu, Z., Gary, E.N., Kim, K.Y., Helble, M., Schultheis, K., Walters, J., Ramos, S., Muthumani, K., Smith, T.R.F., Broderick, K.E., Tebas, P., Patel, A., Weiner, D.B., Kulp, D.W., 2020. J. Clin. Microbiol. 58 https://doi.org/10.1128/JCM.01533-20.

Wang, J., 2021. Cell. Mol. Immunol. 18, 243–244. https://doi.org/10.1038/s41423-020-00584-6.

Wang, J., Jiang, C., Jin, J., Huang, L., Yu, W., Su, B., Hu, J., 2021a. Angew Chem. Int. Ed. Engl. 60, 13042–13049. https://doi.org/10.1002/anie.202103458.

Wang, J.J., Zhang, N., Richardson, S.A., Wu, J.V., 2021b. Expert Rev. Mol. Diagn. 21, 363–370. https://doi.org/10.1080/14737159.2021.1913123.

Zhang, N., Chen, S., Wu, J.V., Yang, X., Wang, J.J., 2020. medRxiv. https://doi.org/10.1101/2020.11.05.20222596, 2020.11.05.20222596.